

TOWARD PREFERENCE-ALIGNED LARGE LANGUAGE MODELS VIA RESIDUAL-BASED MODEL STEERING

Lucio La Cava, Andrea Tagarelli
 DIMES Dept., University of Calabria, Italy
 {lucio.lacava, andrea.tagarelli}@unical.it

ABSTRACT

Preference alignment is a critical step in making Large Language Models (LLMs) useful and aligned with (human) preferences. Existing approaches such as Reinforcement Learning from Human Feedback or Direct Preference Optimization typically require curated data and expensive optimization over billions of parameters, and eventually lead to persistent task-specific models. In this work, we introduce Preference alignment of Large Language Models via Residual Steering (PALRS), a training-free method that exploits preference signals encoded in the residual streams of LLMs. From as few as one hundred preference pairs, PALRS extracts lightweight, plug-and-play steering vectors that can be applied at inference time to push models toward preferred behaviors. We evaluate PALRS on various small-to-medium-scale open-source LLMs, showing that PALRS-aligned models achieve consistent gains on mathematical reasoning and code generation benchmarks while preserving baseline general-purpose performance. Moreover, when compared to DPO-aligned models, they perform better with huge time savings. Our findings highlight that PALRS offers an effective, much more efficient and flexible alternative to standard preference optimization pipelines, offering a training-free, plug-and-play mechanism for alignment with minimal data.

1 INTRODUCTION

Large Language Models (LLMs) have rapidly advanced the state-of-the-art performance across various domains, including dialogue, programming, and mathematical tasks (Li et al., 2025). While most capabilities in such systems are due to rich and wide pretraining (Chen et al., 2024; Kirchenbauer et al., 2024; Shaib et al., 2024; Wang et al., 2025b), a key determinant in their usability is how close their outputs align with *human preferences* (Wang et al., 2023; Shen et al., 2023). Indeed, preference alignment has emerged in recent years as a focal stage in the LLM deployment pipeline: approaches such as reinforcement learning from human feedback (Ouyang et al., 2022; Bai et al., 2022) and direct preference optimization (DPO) (Rafailov et al., 2023) have become standard practices for eliciting better capabilities from LLMs.

Despite their tangible effects, preference-optimization alignment methods remain costly and inflexible. First, current approaches rely on large volumes of curated preference datasets (Köpf et al., 2023), thus being highly *annotation intensive*. Second, despite parameter-efficient methods such as LoRA adapters, aligning a model remains *computationally intensive* because it requires repeated forward and backward passes through large models, often consuming substantial GPU hours. (Stennnon et al., 2020). Third, alignment is typically considered *persistent*: once an LLM has been fine-tuned toward a particular preference setting, adapting it to a different set of preferences generally requires starting again from the base model to produce new checkpoints. Maintaining multiple preference-specific checkpoints can quickly become resource-intensive. These challenges underscore the need to scale alignment methods across three dimensions: efficiency (reducing computational cost), effectiveness (maximizing alignment quality), and flexibility (enabling rapid adaptation to new preference specifications).

Recently, an emerging line of research has unveiled that *residual stream activations* of LLMs encode contextually rich and linearizable features that can be used to manipulate the model behavior surgically, yet without altering their weights or requiring any additional training (Zou et al., 2023; Zhang

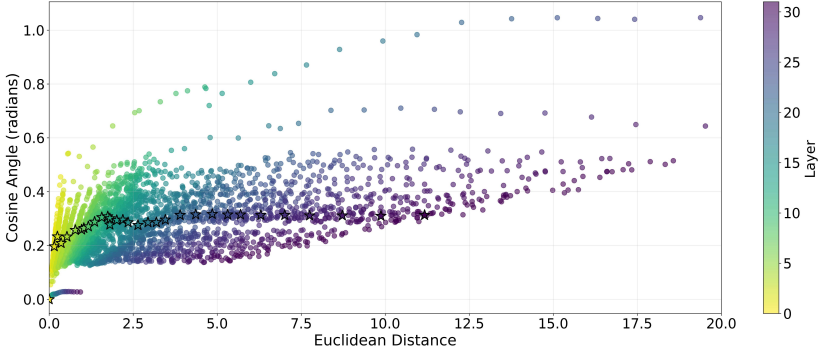


Figure 1: Euclidean distance and cosine angle between residual stream activations (from Llama 3.1 8B Instruct) of pairs of chosen-rejected responses to math questions, for a fixed token position (last position in each input response) and varying model layers. Stars denote average coordinates for each layer. *(Best viewed in color)*

& Nanda, 2024). Residual-based interventions have been shown effective to mitigate refusal behaviors (Arditi et al., 2024; Wang et al., 2025a), erase concepts (Belrose et al., 2023), induce desired persona-like behaviors (Chen et al., 2025), or improve factfulness (Li et al., 2023). These results suggest a promising direction, with residuals functioning as “control knobs,” providing a relatively inexpensive yet effective mechanism for steering model behavior at inference time. However, prior work has focused on optimizing narrow behaviors (e.g., refusal mitigation), leaving the broader challenge of using residual interventions to align models with a range of preferences underexplored.

Our Hypothesis. Consider the task of improving a model’s mathematical reasoning or coding capabilities. Standard practices based on preference optimization alignment, would require curating thousands of preference pairs, optimizing the model’s weights, and deploying task-specific checkpoints, resulting in a resource-intensive and inflexible process.

In this work, we hypothesize that the difference between the residual stream activations of chosen and rejected responses—to questions grounded in a particular domain, e.g., math or coding—can be distilled into steering directions that can be used to induce *preferred behaviors* in a model via lightweight inference-time interventions.

To support our hypothesis, consider Figure 1, which shows Euclidean distance and cosine angle between residual stream activations (from Llama 3.1 8B Instruct) of pairs of chosen-rejected responses to math questions. The observed relatively large Euclidean distances offer evidence that the chosen and rejected activations can be far apart in residual space, which implies the possibility of defining a vector, or steering direction, that moves the activation from the rejected toward the chosen response: if the difference were tiny, a steering vector would have little effect, by contrast, large distances suggest the difference is sufficiently large to guide model behavior adjustment. In addition, the fairly low angles observed in the majority of points offer evidence that the differences between chosen and rejected activations are mostly consistent in direction, thus allowing a generalizable aggregated steering vector to be distilled, rather than needing a separate vector for each example. Combining the two insights, i.e., the chosen-rejected differences are significant in magnitude and relatively coherent in direction, raises a pattern suggesting that a residual-based intervention could reliably guide the model toward preferred behaviors.

Preference alignment of Large Language Models via Residual Steering (PALRS). Building on the above remarks, we introduce a novel approach to preference alignment of LLMs through steering with residual stream activations, dubbed PALRS. Instead of updating model weights via gradient optimization, PALRS identifies preference directions by extracting differences in residual activations from only a small set of preference pairs (on the order of 100). These directions are then applied at inference time, enabling lightweight, plug-and-play steering toward preferred behaviors.

To the best of our knowledge, this is the first study to leverage residual stream directions for preference alignment. Our contributions are threefold:

- We bring the model steering framework based on residual stream activations to the setting of preference alignment of LLMs, showing that residual stream activations encode preference information in a linearly accessible form.
- We introduce a simple difference-in-means approach for estimating candidate preference directions from a small set of chosen–rejected response pairs, without requiring any LLM post-training. We further propose a principled criterion for selecting the steering direction that best aligns an LLM’s behavior with target preferences.
- We demonstrate the effectiveness of PALRS through different small-to-medium scale open-source LLMs, with testing on widely used benchmarks. Particularly, as a concrete case study, we show that steering directions derived from preference-alignment datasets conceived for *math reasoning* (GSM8K) and *code generation* (HumanEval), under certain conditions of the steering intensity, lead an LLM to improve performance on corresponding benchmarks, without degrading results on other-domain benchmarks. Additionally, we highlight that PALRS-aligned models outperform DPO-aligned models on both GSM8K and HumanEval, achieving superior effectiveness while requiring much less computational overhead.

2 METHODOLOGY

2.1 PRELIMINARIES

Notation. Throughout this paper, we will use capital letters to denote data objects, lowercase letters to denote scalars, and bold lowercase letters to denote vectors.

We are given a collection of text triplets $\langle Q, A^{(+)}, A^{(-)} \rangle$ where Q is a question, and A s are two possible (human-provided) answers to Q . Based upon this collection, we define the dataset $\mathcal{D} = \{\langle Q, A^{(+)}, A^{(-)} \rangle \mid A^{(+)} \succ_Q A^{(-)}\}$, where $A^{(+)} \succ_Q A^{(-)}$ denotes that, for question Q , $A^{(+)}$ is preferred over $A^{(-)}$. Let also $\mathbf{t}^{(+)}$, $\mathbf{t}^{(-)}$, and $\mathbf{t}^{(Q)}$ denote the input sequences of tokens from an answer $A^{(+)}$, $A^{(-)}$ ¹ and question Q , respectively.

Residual stream activations. Following previous studies (Zhang & Nanda, 2024), we resort to the concept of *residual stream activation*, specifically in the context of a standard Transformer decoder model, with L layers and hidden size d .

Given an input sequence \mathbf{t} , the state of knowledge a model has about a token in position i at the start of layer ℓ (i.e., before layer ℓ processes it) can effectively be expressed by the token’s residual stream activation, given the input tokens up to position i and all contributions computed from the layers preceding ℓ . We will denote it as a real-valued d -dimensional vector $\mathbf{x}_{i,\ell}(\mathbf{t})$, or simply with $\mathbf{x}_{i,\ell}$ if \mathbf{t} is clear from the context.

In other words, the token’s residual stream activation is the accumulated hidden representation of the token as it flows through the model, thus encoding all contextual information that the model has built up so far—which includes the initial token and positional embeddings, plus the contributions from the multi-head causal self-attention and feed-forward MLP components (sublayers) of all previous layers. This also means that the residual stream is linearly interpretable, since sublayer outputs are added to the residual stream, and is tied to the model’s prediction distribution, since at the final layer the model projects the last residual stream through the embedding-to-token matrix to get the next-token logits.

Model steering. The residual stream activation can be used for model steering because it is the central state vector that encodes all of the model’s knowledge about a token at a given point.

One effective way to reliably alter the model’s outputs and behavior is *activation addition*, i.e., adding an identified direction $\mathbf{r} \in \mathbb{R}^d$ in the residual space that corresponds to some feature, e.g., to

¹The two vectors may have arbitrary and different lengths; however, it will be ensured that any token positions remain consistent across both vectors.

kens that are more representative of the chosen responses than the rejected ones. Therefore, shifting the residual stream along that direction will change the model’s predictions accordingly.

An opposite approach is *directional ablation*, which consists in subtracting from the residual stream its orthogonal projection onto the direction \mathbf{r} . However, as noted in (Arditi et al., 2024), the two approaches have a different impact as the directional ablation applies to all layers and token positions; by contrast, the activation addition involves only a desired layer (and applies across all token positions). Besides that, while ablation has been proven effective in refusal-removal setups (Arditi et al., 2024; Wang et al., 2025a), it is not well-suited to our setting: indeed, chosen and rejected responses typically differ only by a few key tokens, thus ablating their direction is very likely to disrupt the model’s behavior.

2.2 EXTRACTING PREFERENCE DIRECTIONS

To extract the candidate *preference directions* from the model’s residual stream activations, we resort to the *difference-in-means* approach (Belrose, 2023), which has shown to be effective in previous work (Arditi et al., 2024; Tigges et al., 2024; Wang et al., 2025a).

Given the dataset $\mathcal{D} = \{\langle Q, A^{(+)}, A^{(-)} \rangle \mid A^{(+)} \succ_Q A^{(-)}\}$ of triplets of questions and chosen-rejected responses, we first compute two quantities for any choice of token position i and layer ℓ , which correspond to the average of the residual stream activations produced by the model when it receives in input the chosen, resp. rejected, responses:

$$\boldsymbol{\mu}_{i,\ell}^{(+)} = \frac{1}{|\mathcal{D}|} \sum_{A^{(+)} \in \mathcal{D}} \mathbf{x}_{i,\ell}(\mathbf{t}^{(+)}) , \quad \boldsymbol{\mu}_{i,\ell}^{(-)} = \frac{1}{|\mathcal{D}|} \sum_{A^{(-)} \in \mathcal{D}} \mathbf{x}_{i,\ell}(\mathbf{t}^{(-)}). \quad (1)$$

We define the *candidate preference direction* for a given token position i and layer ℓ as the difference between the two means as follows:

$$\mathbf{r}_{i,\ell} = \boldsymbol{\mu}_{i,\ell}^{(+)} - \boldsymbol{\mu}_{i,\ell}^{(-)}. \quad (2)$$

It is worth noticing that, to prevent diluting the residual stream signals, we focus on the chosen and rejected responses while discarding the instruction Q from the computation of directions. Indeed, we are interested in discerning the signals that differentiate the chosen tokens from the rejected ones, regardless of a particular prompt.

Position and layer selection strategies. Following (Arditi et al., 2024), we consider only token positions corresponding to *post-instruction tokens*, i.e., the template tokens following the instruction (e.g., `<|eot_id|>` in Llama 3, cf. Appendix A), ensuring the model processed the given text and starts producing its output.

Regarding the selection of layers, we emphasize the importance of focusing on mid-to-late layers for model steering. The rationale is that early layers primarily shape broad syntactic and structural features, well before semantics, knowledge retrieval, and reasoning processes emerge in the mid layers; also, late layers and especially the unembedding layer directly influence the logits, which bias outputs without meaningfully altering intermediate reasoning.

2.3 SELECTING THE STEERING DIRECTION

Our goal is to choose the vector that can effectively steer the model toward the desired preference-aligned behavior, i.e., favoring human-based preferences in generating responses, while avoiding disruption of its general capabilities.

First, we consider the average signal of residual stream activations induced by the chosen responses from \mathcal{D} . Specifically, for a given layer ℓ , we compute the mean residual stream activation at each selected token position and then take the average across all such positions. We denote this quantity by $\boldsymbol{\mu}_{\ell}^{(+)}$.

Let us denote with $\mathcal{C} = \{(i, \ell)\}$ the set of pairs (token-position, layer id) that are selected as result of the previous stage of position and layer selection. We aim to select the steering direction by finding

the preference vector $\mathbf{r}_{i,\ell}$ (with $(i, \ell) \in \mathcal{C}$) that is most strictly aligned with $\boldsymbol{\mu}_\ell^{(+)}$, that is the vector $\mathbf{r}_{i,\ell}$ that preserves the direction of $\boldsymbol{\mu}_\ell^{(+)}$ exactly, while only boosting its magnitude. This can be accomplished by finding the vector projection of a $\mathbf{r}_{i,\ell}$ onto $\boldsymbol{\mu}_\ell^{(+)}$ with the maximum magnitude, or simply the one maximizing the scalar product with $\boldsymbol{\mu}_\ell^{(+)}$:

$$\mathbf{r}^* = \arg \max_{(i,\ell) \in \mathcal{C}} \left\| \left(\mathbf{r}_{i,\ell} \cdot \frac{\boldsymbol{\mu}_\ell^{(+)}}{\|\boldsymbol{\mu}_\ell^{(+)}\|} \right) \frac{\boldsymbol{\mu}_\ell^{(+)}}{\|\boldsymbol{\mu}_\ell^{(+)}\|} \right\| = \arg \max_{(i,\ell) \in \mathcal{C}} |\mathbf{r}_{i,\ell} \cdot \boldsymbol{\mu}_\ell^{(+)}|. \quad (3)$$

Above, the absolute value ensures that only the magnitude of alignment with $\boldsymbol{\mu}_\ell^{(+)}$ is maximized, thereby avoiding negative contributions that would otherwise diminish $\|\boldsymbol{\mu}_\ell^{(+)}\|$.

Once we have best aligned a preference direction with the one of the mean activations of the chosen responses, we rescale \mathbf{r}^* so that its norm matches $\|\boldsymbol{\mu}_{\ell^*}^{(+)}\|$, where ℓ^* denotes the layer corresponding to one of the selected \mathbf{r}^* :

$$\hat{\mathbf{r}}^* = \frac{\|\boldsymbol{\mu}_{\ell^*}^{(+)}\|}{\|\mathbf{r}^*\|} \cdot \mathbf{r}^*. \quad (4)$$

The above transformation makes the two vectors comparable on the same scale, which allows us to better control the effect of the multiplicative factor in the activation addition step, as described next.

2.4 APPLYING THE STEERING DIRECTION

The selected preference direction \mathbf{r}^* is eventually used to steer the model toward preference-aligned behavior. As discussed in Sect. 2.1, the model steering is performed through activation addition, which means that the selected preference direction is added to the residual stream activations of any newly generated response by the model. Specifically, given an input token sequence \mathbf{t} and by denoting with \mathbf{x}_{ℓ^*} the residual stream activations at any token position and at layer ℓ^* , the steered residuals are defined as follows:

$$\mathbf{x}'_{\ell^*} := \mathbf{x}_{\ell^*}(\mathbf{t}) + \alpha \hat{\mathbf{r}}^*, \quad (5)$$

where $\alpha \in \mathbb{R}^+$ is a coefficient that controls the strength of the steering effect.

2.5 EXPERIMENTAL SETUP

Preference datasets. To demonstrate our proposed PALRS approach, we chose to focus on two particularly informative testbeds for alignment, namely mathematical reasoning and coding. In fact, compared to broad, general-purpose tasks like commonsense reasoning, math reasoning and coding demand precise logical reasoning and adherence to rules—small alignment errors can directly break correctness—and models’ responses can usually be evaluated unambiguously as correct or incorrect.

Within this view, we used the *argilla/distilabel-math-preference-dpo* dataset,² which provides chosen/rejected pairs grounded in mathematical correctness, and *inclusionAI/Ling-Coder-DPO*,³ whose preferences aim at improving correctness in coding generation.

From each dataset, we randomly sampled 100 triplets to construct the collection \mathcal{D} , which we use to compute residual stream activations of chosen and rejected responses. Note that the decision to sample a relatively small number of instances is deliberate, as this is sufficient to capture the difference-in-means signal, in line with findings from related work (Arditi et al., 2024; Wang et al., 2025a). In addition, unlike prior work using residual vectors for refusal ablation (Arditi et al., 2024; Wang et al., 2025a) or personality steering (Chen et al., 2025), our approach does not rely on external cues for sample selection, such as evaluation scores, targeted refusal tokens, or LLMs-as-judges.

Evaluation goals and benchmarks. We define the following evaluation goals:

- **(E1)** – Assessing the performance of PALRS-aligned models against baseline models (i.e., not steered) using two well-established benchmarks for the target tasks: **GSM8K** (Cobbe et al., 2021) for mathematical reasoning and **HumanEval** (Chen et al., 2021) for code generation.

²<https://huggingface.co/datasets/argilla/distilabel-math-preference-dpo>

³<https://huggingface.co/datasets/inclusionAI/Ling-Coder-DPO>

Model	Hugging Face ID	Params	Post-training Strategy	No. Layers
Llama 1B	meta-llama/Llama-3.2-1B-Instruct	1B	SFT + RLHF	16
Llama 3B	meta-llama/Llama-3.2-3B-Instruct	3B	SFT + RLHF	28
Llama 8B	meta-llama/Llama-3.1-8B-Instruct	8B	SFT + RLHF	32
Mistral	mistralai/Mistral-7B-Instruct-v0.3	7B	SFT	32
OLMo	allenai/OLMo-2-1124-7B-Instruct	7B	SFT + DPO + RLVR	32

Table 1: Summary of used LLMs. Post-training strategies are abbreviated as SFT: Supervised Fine-Tuning, RLHF: Reinforcement Learning From Human Feedback, RLVR: Reinforcement Learning with Verifiable Reward, DPO: Direct Preference Optimization.

- **(E2)** – Assessing the performance of PALRS-aligned models on tasks outside the target domains, using five widely adopted benchmarks: **ARC-Challenge** (Bhakthavatsalam et al., 2021) for scientific and commonsense reasoning, **HellaSwag** (Zellers et al., 2019) for physical and social commonsense inference, **MMLU** (Hendrycks et al., 2021) for broad knowledge and multi-task understanding, **TruthfulQA** (Lin et al., 2022) for factuality and truthfulness, and **WinoGrande** (Sakaguchi et al., 2020) for coreference resolution and pronoun disambiguation. By treating these benchmarks as *guardrails*, this evaluation aims to measure whether, and to what extent, PALRS-aligned models for math or coding steering are able to preserve general-purpose capabilities of baseline models.
- **(E3)** – Comparing PALRS-aligned models with DPO-aligned models on the target tasks, using the same 100-sample preference data, and evaluating their performance on the benchmarks as well as their efficiency.
- **(E4)** – Assessing the parameter sensitivity of the steering coefficient and its impact on PALRS in the target tasks.

To ensure reliability and reproducibility in the evaluation of models, we used the well-established **Language Model Evaluation Harness** framework (Gao et al., 2024) via its **TinyBenchmarks** tasks (Polo et al., 2024), which are a curated selection of samples from the aforementioned benchmarks that ensure the same evaluation robustness as the full one, at a reduced temporal cost. The performance results which will be reported for the experiments correspond to *exact_match* for **GSM8K**, *pass@1* for **HumanEval**, and *accuracy* for the remaining benchmarks.

Models. We experimented with a range of LLMs differing in family, post-training strategy, and parameter size, as summarized in Table 1. These include Llama3 (Dubey et al., 2024) in its 1B, 3B, and 8B variants, Mistral (Jiang et al., 2023) 7B, and OLMo2 (OLMo et al., 2025) 7B. This variety enables us to assess to some extent the impact of model architectures, post-training approaches, and sizes on the steering behavior induced by PALRS.

As mentioned in Sect. 2.2, we inspected mid-to-late layers in each of the models. Specifically, we selected a range $[0.3L..0.9L]$, where L is the number of layers as reported in Table 1.

3 RESULTS

Performance of PALRS on target tasks (E1). Looking at the first two result-columns in Table 2,⁴ we observe how PALRS_{Math} systematically boosts the math-related task (GSM8K) across all models, with an average improvement over the baseline around +14% (from +3.7% with OLMo up to +20.1% with Llama 1B). Analogously, PALRS_{Code} consistently improves the code-related task (HumanEval) across all models, with an average improvement over the baseline around +22% (from +2.6% with Llama 8B up to +53.3% with Mistral).

Performance of PALRS on guardrail tasks (E2). Important insights also emerge from the performance over the guardrail benchmarks (right-most five columns in Table 2). PALRS-aligned Llama 1B, Llama 8B, and OLMo are fairly stable, with average percentage changes on guardrail benchmarks around -1% or less—specifically, for PALRS_{Math} resp. PALRS_{Code}, -0.86% resp. +0.35% with Llama 1B, -0.64 resp. -0.08% with Llama 8B, and -0.73% resp. -0.51% with OLMo.

⁴Table 2 reports the results corresponding to the best model configurations for steering direction extraction, as reported in Table 4 in Appendix C.

Tasks		Targets \uparrow		Guardrails \uparrow				
Model	Variant	GSM8K	HumanEval	ARC-C	HellaSwag	MMLU	TruthQA	WinoGrande
Llama 1B	Baseline	0.34	0.38	0.44	0.55	0.43	0.43	0.57
	PALRS_{Math}	0.41 (+20.10%)	0.41 (+7.89%)	0.42 (-3.68%)	0.54 (-1.03%)	0.44 (+2.39%)	0.42 (-2.89%)	0.58 (+0.90%)
	PALRS_{Code}	0.31 (-9.90%)	0.48 (+26.32%)	0.41 (-6.70%)	0.56 (+1.95%)	0.45 (+4.32%)	0.44 (+3.64%)	0.56 (-1.47%)
Llama 3B	Baseline	0.62	0.60	0.57	0.78	0.63	0.48	0.61
	PALRS_{Math}	0.70 (+13.53%)	0.56 (-6.67%)	0.54 (-5.54%)	0.73 (-5.60%)	0.62 (-0.85%)	0.45 (-5.61%)	0.62 (+1.61%)
	PALRS_{Code}	0.57 (-7.72%)	0.67 (+11.67%)	0.55 (-3.66%)	0.74 (-5.19%)	0.61 (-2.89%)	0.48 (-0.39%)	0.64 (+4.52%)
Llama 8B	Baseline	0.72	0.78	0.65	0.81	0.63	0.54	0.75
	PALRS_{Math}	0.82 (+13.09%)	0.77 (-1.28%)	0.63 (-3.32%)	0.81 (+0.32%)	0.63 (-0.12%)	0.55 (+1.62%)	0.73 (-1.71%)
	PALRS_{Code}	0.76 (+4.71%)	0.80 (+2.56%)	0.65 (-0.52%)	0.81 (+0.00%)	0.63 (-0.58%)	0.54 (+0.18%)	0.75 (+0.50%)
Mistral	Baseline	0.45	0.15	0.64	0.84	0.64	0.61	0.76
	PALRS_{Math}	0.53 (+18.42%)	0.15 (+0.00%)	0.65 (+1.64%)	0.84 (-0.05%)	0.64 (-0.19%)	0.61 (-0.09%)	0.76 (+0.00%)
	PALRS_{Code}	0.47 (+3.84%)	0.23 (+53.33%)	0.65 (+0.95%)	0.84 (+0.02%)	0.64 (-0.10%)	0.61 (-1.46%)	0.75 (-1.31%)
OLMo	Baseline	0.75	0.52	0.66	0.83	0.62	0.56	0.76
	PALRS_{Math}	0.77 (+3.71%)	0.53 (+1.92%)	0.65 (-1.19%)	0.83 (-0.18%)	0.61 (-1.51%)	0.54 (-2.43%)	0.77 (+0.72%)
	PALRS_{Code}	0.78 (+4.88%)	0.60 (+15.38%)	0.66 (+0.26%)	0.83 (+0.17%)	0.62 (+0.00%)	0.55 (-1.71%)	0.75 (-1.28%)

Table 2: Benchmark performance results: Baseline vs. PALRS-aligned models. Bold values correspond to PALRS-aligned model performances on the target tasks. Values in parenthesis indicate percentage increase of a PALRS-aligned model w.r.t. the baseline performance on the same task.

$\text{PALRS}_{\text{Math}}$ with Mistral even slightly improves on average over the guardrails (+0.26%), while keeping average guardrail degradation around -0.38% when using $\text{PALRS}_{\text{Code}}$. By contrast, Llama 3B is the only model to suffer the most guardrail degradation, up to -3.19% with $\text{PALRS}_{\text{Math}}$.

Focusing on the models, Mistral provides the largest boost by $\text{PALRS}_{\text{Code}}$ (+53.4%) and second large by $\text{PALRS}_{\text{Math}}$ (+18.4%). Using Llama models has shown a scaling effect, since smaller models lead to relative larger gains but also stronger impact on guardrail tasks. By contrast, PALRS-aligned OLMo models have the least improvement (+3.7%) over the baseline on the math task, but a significant +15.4% on the coding task.

Remarkably, PALRS alignment of the largest models, i.e., OLMo, Mistral and Llama 8B, on one target task reveals little degradation or, more often, improvement over the other target task, suggesting that steering in particular on a math task can have beneficial effect on a coding task as well.

Comparison of PALRS with DPO (E3). Figure 2 compares PALRS-aligned models with DPO-aligned models, in terms of effectiveness and efficiency on the **GSM8K** and **HumanEval** benchmarks (cf. Appendix B for details on the hardware used). $\text{PALRS}_{\text{Math}}$ -aligned models always outperform the corresponding DPO-aligned on **GSM8K**: we notice a clear percentage increase consistently over all models, ranging from +2.6% with OLMo to +20.5% with Mistral, with an average gain of +10.4%, thus showing robustness across model-scales.

This couples with another outstanding result, which regards time efficiency: $\text{PALRS}_{\text{Math}}$ -aligned models are an order of magnitude faster than the corresponding DPO-aligned on **GSM8K**. For example, on Llama 3B, learning the $\text{PALRS}_{\text{Math}}$ -aligned model takes about 31s vs. DPO-aligned

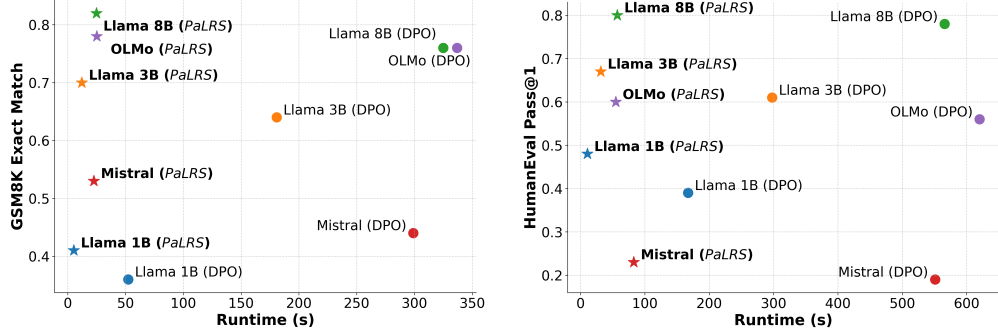


Figure 2: Benchmark performance and efficiency comparison of PALRS- and DPO-aligned models: GSM8K (left) and HumanEval (right). Colored points denote models, star resp. circle markers denote PALRS- resp DPO-alignment.

one’s 300s, i.e., $\sim 10x$ faster. It is also worth emphasizing that, as models grow larger, DPO-aligned models’ times increase steeply, while PALRS_{Math}-aligned models scale much more smoothly (from 5s to about 25s). Accuracy also scales better with PALRS_{Math}-aligned models: the performance gap against DPO widens with larger models.

Analogous remarks can be drawn from the comparison on the HumanEval benchmark. The performance gain of PALRS vs. DPO here is from +2.6% (Llama 8B) to 23.1% (Llama 1B), and tends to diminish as models get larger, again except for Mistral, whereby PALRS_{Code} model has a percentage increase of +21%. Also, PALRS_{Code}-aligned models are again an order of magnitude faster than corresponding DPO models, with an average speedup of 10x across models, and the time gap increases linearly with model size, showing PALRS_{Code}-aligned models are far more scalable.

Impact of the steering coefficient (E4). We investigate the sensitivity of the steering coefficient α (cf. Eq. (5)) and its effect on the performance of PALRS-aligned models on the target tasks. Figure 3 provides insights which can be summarized as follows. We notice that the coefficient sensitivity is model- and task-dependent. While in general performance trends drop consistently as the coefficient increases, there is always a regime of the coefficient where the PALRS-aligned models outperform the relative baselines. Low to moderate coefficients (up to 0.8) often yield the best trade-offs, especially for Llama 3B, Llama 8B (GSM8K) and OLMo (HumanEval). Oversteering is most visible at coefficient at 1.0 for all models. More specifically, for Llama 3B and OLMo (HumanEval), the beneficial range is around 0.6–0.8 before oversteering occurs; for Mistral and Llama 1B, oversteering happens much earlier (as low as 0.4–0.6), while Llama 8B tolerates higher coefficients better but still show oversteering when pushed too far. To sum up, steering shows to be beneficial, but needs moderate tuning of the coefficient to avoid oversteering and performance degradation.

4 RELATED WORK

Model Steering via Feature Directions. Recent studies suggest that linear directions in the activation space of LLMs capture richer and more generalizable features than individual neurons (Bolukbasi et al., 2016; Li et al., 2021; Elhage et al., 2022). This shift toward subspace-level aspects has motivated research that exploits linear representations to probe model internals and provide better interpretation and steering of their behaviors (Hernandez & Andreas, 2021; Nanda et al., 2023; Park et al., 2024). A key challenge is to reliably identify such feature directions. In this regard, unsupervised approaches based on Sparse Auto-Encoders (SAE) have been used to uncover latent, interpretable features (Huben et al., 2024; Lan et al., 2024; Shu et al., 2025). A complementary trend involves exploiting contrastive pairs of texts differing across a specific axis (e.g., sentiment) to extract directions that isolate targeted behaviors (Burns et al., 2023; Rimsky et al., 2024).

Once extracted, these features can be used to intervene on model activations, particularly in the residual stream, where editing is known to effectively steer the models’ behavior (Zou et al., 2023; Zhang & Nanda, 2024). Such interventions have been shown promising in shifting sentiment and

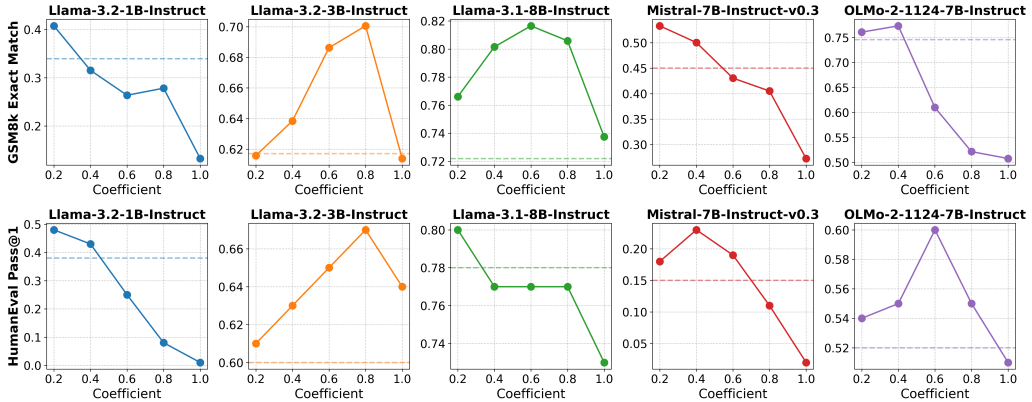


Figure 3: Performance of PALRS-aligned models on the target tasks **GSM8K** (top) and **HumanEval** (bottom) by varying the steering coefficient. Dashed horizontal line marks the baseline performance.

detoxification (Turner et al., 2023), enhancing truthfulness (Li et al., 2023), erasing concepts (Belrose et al., 2023), targeting refusal behaviors (Arditi et al., 2024; Wang et al., 2025a), and controlling character traits in LLMs Chen et al. (2025).

Preference Optimization in LLMs. A large body of work has focused on aligning LLMs with human preferences, aiming to render such tools more usable Wang et al. (2023); Shen et al. (2023). This has been largely driven by Reinforcement Learning from Human Feedback (RLHF) approaches (Ouyang et al., 2022; Bai et al., 2022), and more efficient methods like Direct Preference Optimization (DPO) (Rafailov et al., 2023). Nonetheless, despite recent efforts to further improve efficiency (Hong et al., 2024; Meng et al., 2024), the promising and more efficient alternative of steering models toward preferences via residual streams remained almost totally unexplored.

In a related effort, a recent work by Liu et al. (2024) explores preference alignment by identifying disparities in activation patterns elicited by preferred versus dispreferred stimuli. While this represents an important step toward bridging preference data with internal model representations, their approach differs fundamentally from ours. First, it requires training with contrastive stimuli to extract the relevant signals, whereas our method is entirely *training-free*. Second, it introduces a low-rank adaptation module to perform steering, in contrast to our *inference-time intervention*. These design choices also manifest in practice, as their method yields more limited steering effects compared to the lightweight and scalable improvements enabled by PALRS.

5 CONCLUSIONS

In this work, we presented PALRS, a training-free method for preference alignment that leverages residual stream activations to steer LLM behavior directly at inference time. By distilling steering vectors from as few as a hundred preference pairs, PALRS aligns models with desired behaviors without any parameter updates, costly optimization, or the need to maintain multiple fine-tuned checkpoints. Crucially, our results show that PALRS-aligned models are a safer and consistently superior alternative to their DPO-aligned counterparts: never underperforming, often achieving substantial gains, and doing so with orders-of-magnitude less computation. Our findings render residual-based steering as a powerful paradigm for preference alignment, aiming to make it simpler, more effective yet scalable, and broadly accessible compared to traditional post-training approaches.

Limitations. While our results highlight the promise of residual-based preference alignment, several limitations remain. First, although we evaluated PALRS on a relatively representative sample of model families and post-training modalities, its generalizability to larger-scale or proprietary models needs to be evaluated. Second, our current method for discovering effective data subsets and steering coefficients relies on heuristic grid search: developing principled, theoretically grounded selection strategies remains a key direction for smoother real-world deployment of our results. Third, while our results demonstrate that residual interventions effectively steer model behavior and provide em-

pirical support for our hypothesis, more in-depth explainability of how preference information is encoded and disentangled across layers is needed. Overall, we demonstrate the feasibility of this approach, while leaving refinement and addressing these limitations to future research.

ETHICS STATEMENTS

Our work demonstrates that residual-based preference steering can effectively influence model behavior. While this highlights the potential for beneficial applications, we acknowledge that such methods might also be misused to steer models toward harmful or malicious behaviors. We strongly discourage any such misuse and do not assume responsibility for applications beyond the scope of this research. We encourage researchers and practitioners within this research area to adhere to established safety and ethical guidelines when applying our proposed technique or related ones, and to prioritize transparency, fairness, and safety of end users.

Reproducibility Statement. We are strongly committed to ensuring reproducibility of our results. All experimental settings, hyperparameters, and model configurations are provided in detail in the paper. The code associated with this submission will be released upon acceptance.

REFERENCES

- Andy Arditi, Oscar Obeso, Aaquib Syed, Daniel Paleka, Nina Panickssery, Wes Gurnee, and Neel Nanda. Refusal in language models is mediated by a single direction. In Amir Globersons, Lester Mackey, Danielle Belgrave, Angela Fan, Ulrich Paquet, Jakub M. Tomczak, and Cheng Zhang (eds.), *Advances in Neural Information Processing Systems 38: Annual Conference on Neural Information Processing Systems 2024, NeurIPS 2024, Vancouver, BC, Canada, December 10 - 15, 2024, 2024*. URL http://papers.nips.cc/paper_files/paper/2024/hash/f545448535dfde4f9786555403ab7c49-Abstract-Conference.html.
- Yuntao Bai, Andy Jones, Kamal Ndousse, Amanda Askell, Anna Chen, Nova DasSarma, Dawn Drain, Stanislav Fort, Deep Ganguli, Tom Henighan, Nicholas Joseph, Saurav Kadavath, Jackson Kernion, Tom Conerly, Sheer El Showk, Nelson Elhage, Zac Hatfield-Dodds, Danny Hernandez, Tristan Hume, Scott Johnston, Shauna Kravec, Liane Lovitt, Neel Nanda, Catherine Olsson, Dario Amodei, Tom B. Brown, Jack Clark, Sam McCandlish, Chris Olah, Benjamin Mann, and Jared Kaplan. Training a helpful and harmless assistant with reinforcement learning from human feedback. *CoRR*, abs/2204.05862, 2022. doi: 10.48550/ARXIV.2204.05862. URL <https://doi.org/10.48550/arXiv.2204.05862>.
- Nora Belrose. Diff-in-means concept editing is worst-case optimal: Explaining a result by Sam Marks and Max Tegmark, 2023. <https://blog.eleuther.ai/diff-in-means/>. Accessed on: May 20, 2024.
- Nora Belrose, David Schneider-Joseph, Shauli Ravfogel, Ryan Cotterell, Edward Raff, and Stella Biderman. LEACE: perfect linear concept erasure in closed form. In Alice Oh, Tristan Naumann, Amir Globerson, Kate Saenko, Moritz Hardt, and Sergey Levine (eds.), *Advances in Neural Information Processing Systems 36: Annual Conference on Neural Information Processing Systems 2023, NeurIPS 2023, New Orleans, LA, USA, December 10 - 16, 2023, 2023*. URL http://papers.nips.cc/paper_files/paper/2023/hash/d066d21c619d0a78c5b557fa3291a8f4-Abstract-Conference.html.
- Sumithra Bhakthavatsalam, Daniel Khashabi, Tushar Khot, Bhavana Dalvi Mishra, Kyle Richardson, Ashish Sabharwal, Carissa Schoenick, Oyvind Tafjord, and Peter Clark. Think you have solved direct-answer question answering? try arc-da, the direct-answer AI2 reasoning challenge. *CoRR*, abs/2102.03315, 2021. URL <https://arxiv.org/abs/2102.03315>.
- Tolga Bolukbasi, Kai-Wei Chang, James Y. Zou, Venkatesh Saligrama, and Adam Tauman Kalai. Man is to computer programmer as woman is to homemaker? debiasing word embeddings. In Daniel D. Lee, Masashi Sugiyama, Ulrike von Luxburg, Isabelle Guyon, and Roman Garnett (eds.), *Advances in Neural Information Processing Systems 29: Annual Conference on Neural Information Processing Systems 2016, December 5-10, 2016, Barcelona, Spain*, pp.

4349–4357, 2016. URL <https://proceedings.neurips.cc/paper/2016/hash/a486cd07e4ac3d270571622f4f316ec5-Abstract.html>.

Collin Burns, Haotian Ye, Dan Klein, and Jacob Steinhardt. Discovering latent knowledge in language models without supervision. In *The Eleventh International Conference on Learning Representations, ICLR 2023, Kigali, Rwanda, May 1-5, 2023*. OpenReview.net, 2023. URL <https://openreview.net/forum?id=ETKGuby0hcs>.

Mark Chen, Jerry Tworek, Heewoo Jun, Qiming Yuan, Henrique Pondé de Oliveira Pinto, Jared Kaplan, Harri Edwards, Yuri Burda, Nicholas Joseph, Greg Brockman, Alex Ray, Raul Puri, Gretchen Krueger, Michael Petrov, Heidy Khlaaf, Girish Sastry, Pamela Mishkin, Brooke Chan, Scott Gray, Nick Ryder, Mikhail Pavlov, Alethea Power, Lukasz Kaiser, Mohammad Bavarian, Clemens Winter, Philippe Tillet, Felipe Petroski Such, Dave Cummings, Matthias Plappert, Fotios Chantzis, Elizabeth Barnes, Ariel Herbert-Voss, William Hebgen Guss, Alex Nichol, Alex Paino, Nikolas Tezak, Jie Tang, Igor Babuschkin, Suchir Balaji, Shantanu Jain, William Saunders, Christopher Hesse, Andrew N. Carr, Jan Leike, Joshua Achiam, Vedant Misra, Evan Morikawa, Alec Radford, Matthew Knight, Miles Brundage, Mira Murati, Katie Mayer, Peter Welinder, Bob McGrew, Dario Amodei, Sam McCandlish, Ilya Sutskever, and Wojciech Zaremba. Evaluating large language models trained on code. *CoRR*, abs/2107.03374, 2021. URL <https://arxiv.org/abs/2107.03374>.

Runjin Chen, Andy Ardit, Henry Sleight, Owain Evans, and Jack Lindsey. Persona vectors: Monitoring and controlling character traits in language models. *arXiv preprint arXiv:2507.21509*, 2025.

Yanda Chen, Chen Zhao, Zhou Yu, Kathleen McKeown, and He He. Parallel structures in pre-training data yield in-context learning. In Lun-Wei Ku, Andre Martins, and Vivek Srikumar (eds.), *Proceedings of the 62nd Annual Meeting of the Association for Computational Linguistics (Volume 1: Long Papers)*, pp. 8582–8592, Bangkok, Thailand, August 2024. Association for Computational Linguistics. doi: 10.18653/v1/2024.acl-long.465. URL <https://aclanthology.org/2024.acl-long.465>.

Karl Cobbe, Vineet Kosaraju, Mohammad Bavarian, Mark Chen, Heewoo Jun, Lukasz Kaiser, Matthias Plappert, Jerry Tworek, Jacob Hilton, Reiichiro Nakano, Christopher Hesse, and John Schulman. Training verifiers to solve math word problems. *CoRR*, abs/2110.14168, 2021. URL <https://arxiv.org/abs/2110.14168>.

Abhimanyu Dubey, Abhinav Jauhri, Abhinav Pandey, Abhishek Kadian, Ahmad Al-Dahle, Aiesha Letman, Akhil Mathur, Alan Schelten, Amy Yang, Angela Fan, Anirudh Goyal, Anthony Hartshorn, Aobo Yang, Archi Mitra, Archie Sravankumar, Artem Korenev, Arthur Hinsvark, Arun Rao, Aston Zhang, Aurélien Rodriguez, Austen Gregerson, Ava Spataru, Baptiste Rozière, Bethany Biron, Binh Tang, Bobbie Chern, Charlotte Caucheteux, Chaya Nayak, Chloe Bi, Chris Marra, Chris McConnell, Christian Keller, Christophe Touret, Chunyang Wu, Corinne Wong, Cristian Canton Ferrer, Cyrus Nikolaidis, Damien Allonsius, Daniel Song, Danielle Pintz, Danny Livshits, David Esiobu, Dhruv Choudhary, Dhruv Mahajan, Diego Garcia-Olano, Diego Perino, Dieuwke Hupkes, Egor Lakomkin, Ehab AlBadawy, Elina Lobanova, Emily Dinan, Eric Michael Smith, Filip Radenovic, Frank Zhang, Gabriel Synnaeve, Gabrielle Lee, Georgia Lewis Anderson, Graeme Nail, Grégoire Mialon, Guan Pang, Guillem Cucurell, Hailey Nguyen, Hannah Korevaar, Hu Xu, Hugo Touvron, Iliyan Zarov, Imanol Arrieta Ibarra, Isabel M. Kloumann, Ishan Misra, Ivan Evtimov, Jade Copet, Jaewon Lee, Jan Geffert, Jana Vranes, Jason Park, Jay Mhadokar, Jeet Shah, Jelmer van der Linde, Jennifer Billock, Jenny Hong, Jenya Lee, Jeremy Fu, Jianfeng Chi, Jianyu Huang, Jiawen Liu, Jie Wang, Jiecao Yu, Joanna Bitton, Joe Spisak, Jongsoo Park, Joseph Rocca, Joshua Johnstun, Joshua Saxe, Junteng Jia, Kalyan Vasuden Alwala, Kartikeya Upasani, Kate Plawiak, Ke Li, Kenneth Heafield, Kevin Stone, and et al. The llama 3 herd of models. *CoRR*, abs/2407.21783, 2024. doi: 10.48550/ARXIV.2407.21783. URL <https://doi.org/10.48550/arXiv.2407.21783>.

Nelson Elhage, Tristan Hume, Catherine Olsson, Nicholas Schiefer, Tom Henighan, Shauna Kravec, Zac Hatfield-Dodds, Robert Lasenby, Dawn Drain, Carol Chen, Roger B. Grosse, Sam McCandlish, Jared Kaplan, Dario Amodei, Martin Wattenberg, and Christopher Olah. Toy models of superposition. *CoRR*, abs/2209.10652, 2022. doi: 10.48550/ARXIV.2209.10652. URL <https://doi.org/10.48550/arXiv.2209.10652>.

Leo Gao, Jonathan Tow, Baber Abbasi, Stella Biderman, Sid Black, Anthony DiPofi, Charles Foster, Laurence Golding, Jeffrey Hsu, Alain Le Noac'h, Haonan Li, Kyle McDonell, Niklas Muenninghoff, Chris Ociepa, Jason Phang, Laria Reynolds, Hailey Schoelkopf, Aviya Skowron, Lintang Sutawika, Eric Tang, Anish Thite, Ben Wang, Kevin Wang, and Andy Zou. The language model evaluation harness, 07 2024. URL <https://zenodo.org/records/12608602>.

Dan Hendrycks, Collin Burns, Steven Basart, Andy Zou, Mantas Mazeika, Dawn Song, and Jacob Steinhardt. Measuring massive multitask language understanding. In *9th International Conference on Learning Representations, ICLR 2021, Virtual Event, Austria, May 3-7, 2021*. OpenReview.net, 2021. URL <https://openreview.net/forum?id=d7KBjmI3GmQ>.

Evan Hernandez and Jacob Andreas. The low-dimensional linear geometry of contextualized word representations. In Arianna Bisazza and Omri Abend (eds.), *Proceedings of the 25th Conference on Computational Natural Language Learning*, pp. 82–93, Online, November 2021. Association for Computational Linguistics. doi: 10.18653/v1/2021.conll-1.7. URL <https://aclanthology.org/2021.conll-1.7/>.

Jiwoo Hong, Noah Lee, and James Thorne. ORPO: Monolithic preference optimization without reference model. In Yaser Al-Onaizan, Mohit Bansal, and Yun-Nung Chen (eds.), *Proceedings of the 2024 Conference on Empirical Methods in Natural Language Processing*, pp. 11170–11189, Miami, Florida, USA, November 2024. Association for Computational Linguistics. doi: 10.18653/v1/2024.emnlp-main.626. URL <https://aclanthology.org/2024.emnlp-main.626/>.

Robert Huben, Hoagy Cunningham, Logan Riggs Smith, Aidan Ewart, and Lee Sharkey. Sparse autoencoders find highly interpretable features in language models. In *The Twelfth International Conference on Learning Representations, ICLR 2024, Vienna, Austria, May 7-11, 2024*. OpenReview.net, 2024. URL <https://openreview.net/forum?id=F76bwRSLeK>.

Albert Q. Jiang, Alexandre Sablayrolles, Arthur Mensch, Chris Bamford, Devendra Singh Chaplot, Diego de Las Casas, Florian Bressand, Gianna Lengyel, Guillaume Lample, Lucile Saulnier, Lélio Renard Lavaud, Marie-Anne Lachaux, Pierre Stock, Teven Le Scao, Thibaut Lavril, Thomas Wang, Timothée Lacroix, and William El Sayed. Mistral 7b. *CoRR*, abs/2310.06825, 2023. doi: 10.48550/ARXIV.2310.06825. URL <https://doi.org/10.48550/arXiv.2310.06825>.

John Kirchenbauer, Garrett Honke, Gowthami Somepalli, Jonas Geiping, Daphne Ippolito, Katherine Lee, Tom Goldstein, and David Andre. LMD3: language model data density dependence. *CoRR*, abs/2405.06331, 2024. doi: 10.48550/ARXIV.2405.06331. URL <https://doi.org/10.48550/arXiv.2405.06331>.

Andreas Köpf, Yannic Kilcher, Dimitri von Rütte, Sotiris Anagnostidis, Zhi Rui Tam, Keith Stevens, Abdullah Barhoum, Duc Nguyen, Oliver Stanley, Richárd Nagyfi, Shahul ES, Sameer Suri, David Glushkov, Arnav Dantuluri, Andrew Maguire, Christoph Schuhmann, Huu Nguyen, and Alexander Mattick. Openassistant conversations - democratizing large language model alignment. In Alice Oh, Tristan Naumann, Amir Globerson, Kate Saenko, Moritz Hardt, and Sergey Levine (eds.), *Advances in Neural Information Processing Systems 36: Annual Conference on Neural Information Processing Systems 2023, NeurIPS 2023, New Orleans, LA, USA, December 10 - 16, 2023*, 2023. URL http://papers.nips.cc/paper_files/paper/2023/hash/949f0f8f32267d297c2d4e3ee10a2e7e-Abstract-Datasets_and_Benchmarks.html.

Michael Lan, Philip Torr, Austin Meek, Ashkan Khakzar, David Krueger, and Fazl Barez. Quantifying feature space universality across large language models via sparse autoencoders. *arXiv preprint arXiv:2410.06981*, 2024.

Belinda Z. Li, Maxwell Nye, and Jacob Andreas. Implicit representations of meaning in neural language models. In Chengqing Zong, Fei Xia, Wenjie Li, and Roberto Navigli (eds.), *Proceedings of the 59th Annual Meeting of the Association for Computational Linguistics and the 11th International Joint Conference on Natural Language Processing (Volume 1: Long Papers)*, pp. 1813–1827, Online, August 2021. Association for Computational Linguistics. doi: 10.18653/v1/2021.acl-long.143. URL <https://aclanthology.org/2021.acl-long.143/>.

Jiawei Li, Yang Gao, Yizhe Yang, Yu Bai, Xiaofeng Zhou, Yinghao Li, Huashan Sun, Yuhang Liu, Xingpeng Si, Yuhao Ye, Yixiao Wu, Yiguan Lin, Bin Xu, Bowen Ren, Chong Feng, and Heyan Huang. Fundamental capabilities and applications of large language models: A survey. *ACM Comput. Surv.*, 58(2), September 2025. ISSN 0360-0300. doi: 10.1145/3735632. URL <https://doi.org/10.1145/3735632>.

Kenneth Li, Oam Patel, Fernanda B. Viégas, Hanspeter Pfister, and Martin Wattenberg. Inference-time intervention: Eliciting truthful answers from a language model. In Alice Oh, Tristan Naumann, Amir Globerson, Kate Saenko, Moritz Hardt, and Sergey Levine (eds.), *Advances in Neural Information Processing Systems 36: Annual Conference on Neural Information Processing Systems 2023, NeurIPS 2023, New Orleans, LA, USA, December 10 - 16, 2023*, 2023. URL http://papers.nips.cc/paper_files/paper/2023/hash/81b8390039b7302c909cb769f8b6cd93-Abstract-Conference.html.

Stephanie Lin, Jacob Hilton, and Owain Evans. TruthfulQA: Measuring how models mimic human falsehoods. In Smaranda Muresan, Preslav Nakov, and Aline Villavicencio (eds.), *Proceedings of the 60th Annual Meeting of the Association for Computational Linguistics (Volume 1: Long Papers)*, pp. 3214–3252, Dublin, Ireland, May 2022. Association for Computational Linguistics. doi: 10.18653/v1/2022.acl-long.229. URL <https://aclanthology.org/2022.acl-long.229/>.

Wenhai Liu, Xiaohua Wang, Muling Wu, Tianlong Li, Changze Lv, Zixuan Ling, Zhu JianHao, Cenyuan Zhang, Xiaoqing Zheng, and Xuanjing Huang. Aligning large language models with human preferences through representation engineering. In Lun-Wei Ku, Andre Martins, and Vivek Srikumar (eds.), *Proceedings of the 62nd Annual Meeting of the Association for Computational Linguistics (Volume 1: Long Papers)*, pp. 10619–10638, Bangkok, Thailand, August 2024. Association for Computational Linguistics. doi: 10.18653/v1/2024.acl-long.572. URL <https://aclanthology.org/2024.acl-long.572/>.

Yu Meng, Mengzhou Xia, and Danqi Chen. Simpo: Simple preference optimization with a reference-free reward. In Amir Globersons, Lester Mackey, Danielle Belgrave, Angela Fan, Ulrich Paquet, Jakub M. Tomczak, and Cheng Zhang (eds.), *Advances in Neural Information Processing Systems 38: Annual Conference on Neural Information Processing Systems 2024, NeurIPS 2024, Vancouver, BC, Canada, December 10 - 15, 2024*, 2024. URL http://papers.nips.cc/paper_files/paper/2024/hash/e099c1c9699814af0be873a175361713-Abstract-Conference.html.

Neel Nanda, Andrew Lee, and Martin Wattenberg. Emergent linear representations in world models of self-supervised sequence models. In Yonatan Belinkov, Sophie Hao, Jaap Jumelet, Najoong Kim, Arya McCarthy, and Hosein Mohebbi (eds.), *Proceedings of the 6th BlackboxNLP Workshop: Analyzing and Interpreting Neural Networks for NLP*, pp. 16–30, Singapore, December 2023. Association for Computational Linguistics. doi: 10.18653/v1/2023.blackboxnlp-1.2. URL <https://aclanthology.org/2023.blackboxnlp-1.2/>.

Team OLMo, Pete Walsh, Luca Soldaini, Dirk Groeneveld, Kyle Lo, Shane Arora, Akshita Bhagia, Yuling Gu, Shengyi Huang, Matt Jordan, Nathan Lambert, Dustin Schwenk, Oyvind Tafjord, Taira Anderson, David Atkinson, Faeze Brahman, Christopher Clark, Pradeep Dasigi, Nouha Dziri, Michal Guerquin, Hamish Ivison, Pang Wei Koh, Jiacheng Liu, Saumya Malik, William Merrill, Lester James V. Miranda, Jacob Morrison, Tyler Murray, Crystal Nam, Valentina Pyatkin, Aman Rangapur, Michael Schmitz, Sam Skjonsberg, David Wadden, Christopher Wilhelm, Michael Wilson, Luke Zettlemoyer, Ali Farhadi, Noah A. Smith, and Hannaneh Hajishirzi. 2 olmo 2 furious. *CoRR*, abs/2501.00656, 2025. doi: 10.48550/ARXIV.2501.00656. URL <https://doi.org/10.48550/arXiv.2501.00656>.

Long Ouyang, Jeffrey Wu, Xu Jiang, Diogo Almeida, Carroll L. Wainwright, Pamela Mishkin, Chong Zhang, Sandhini Agarwal, Katarina Slama, Alex Ray, John Schulman, Jacob Hilton, Fraser Kelton, Luke Miller, Maddie Simens, Amanda Askell, Peter Welinder, Paul F. Christiano, Jan Leike, and Ryan Lowe. Training language models to follow instructions with human feedback. In Sanmi Koyejo, S. Mohamed, A. Agarwal, Danielle Belgrave, K. Cho, and A. Oh (eds.), *Advances in Neural Information Processing Systems 35: Annual Conference on Neural Information Processing Systems 2022, NeurIPS 2022, New Orleans, LA, USA, November 28 - December*

- 9, 2022, 2022. URL http://papers.nips.cc/paper_files/paper/2022/hash/b1efde53be364a73914f58805a001731-Abstract-Conference.html.
- Kiho Park, Yo Joong Choe, and Victor Veitch. The linear representation hypothesis and the geometry of large language models. In *Forty-first International Conference on Machine Learning, ICML 2024, Vienna, Austria, July 21-27, 2024*. OpenReview.net, 2024. URL <https://openreview.net/forum?id=UGpGkLzwpP>.
- Felipe Maia Polo, Lucas Weber, Leshem Choshen, Yuekai Sun, Gongjun Xu, and Mikhail Yurochkin. tinybenchmarks: evaluating llms with fewer examples. In *Forty-first International Conference on Machine Learning, ICML 2024, Vienna, Austria, July 21-27, 2024*. OpenReview.net, 2024. URL <https://openreview.net/forum?id=qAml3FpfhG>.
- Rafael Rafailov, Archit Sharma, Eric Mitchell, Christopher D. Manning, Stefano Ermon, and Chelsea Finn. Direct preference optimization: Your language model is secretly a reward model. In Alice Oh, Tristan Naumann, Amir Globerson, Kate Saenko, Moritz Hardt, and Sergey Levine (eds.), *Advances in Neural Information Processing Systems 36: Annual Conference on Neural Information Processing Systems 2023, NeurIPS 2023, New Orleans, LA, USA, December 10 - 16, 2023*, 2023. URL http://papers.nips.cc/paper_files/paper/2023/hash/a85b405ed65c6477a4fe8302b5e06ce7-Abstract-Conference.html.
- Nina Rimsky, Nick Gabrieli, Julian Schulz, Meg Tong, Evan Hubinger, and Alexander Turner. Steering llama 2 via contrastive activation addition. In Lun-Wei Ku, Andre Martins, and Vivek Srikumar (eds.), *Proceedings of the 62nd Annual Meeting of the Association for Computational Linguistics (Volume 1: Long Papers)*, pp. 15504–15522, Bangkok, Thailand, August 2024. Association for Computational Linguistics. doi: 10.18653/v1/2024.acl-long.828. URL <https://aclanthology.org/2024.acl-long.828/>.
- Keisuke Sakaguchi, Ronan Le Bras, Chandra Bhagavatula, and Yejin Choi. Winogrande: An adversarial winograd schema challenge at scale. In *The Thirty-Fourth AAAI Conference on Artificial Intelligence, AAAI 2020, The Thirty-Second Innovative Applications of Artificial Intelligence Conference, IAAI 2020, The Tenth AAAI Symposium on Educational Advances in Artificial Intelligence, EAAI 2020, New York, NY, USA, February 7-12, 2020*, pp. 8732–8740. AAAI Press, 2020. doi: 10.1609/AAAI.V34I05.6399. URL <https://doi.org/10.1609/aaai.v34i05.6399>.
- Chantal Shaib, Yanai Elazar, Junyi Jessy Li, and Byron C Wallace. Detection and measurement of syntactic templates in generated text. In Yaser Al-Onaizan, Mohit Bansal, and Yun-Nung Chen (eds.), *Proceedings of the 2024 Conference on Empirical Methods in Natural Language Processing*, pp. 6416–6431, Miami, Florida, USA, November 2024. Association for Computational Linguistics. doi: 10.18653/v1/2024.emnlp-main.368. URL <https://aclanthology.org/2024.emnlp-main.368/>.
- Tianhao Shen, Renren Jin, Yufei Huang, Chuang Liu, Weilong Dong, Zishan Guo, Xinwei Wu, Yan Liu, and Deyi Xiong. Large language model alignment: A survey. *CoRR*, abs/2309.15025, 2023. doi: 10.48550/ARXIV.2309.15025. URL <https://doi.org/10.48550/arXiv.2309.15025>.
- Dong Shu, Xuansheng Wu, Haiyan Zhao, Daking Rai, Ziyu Yao, Ninghao Liu, and Mengnan Du. A survey on sparse autoencoders: Interpreting the internal mechanisms of large language models. *CoRR*, abs/2503.05613, 2025. doi: 10.48550/ARXIV.2503.05613. URL <https://doi.org/10.48550/arXiv.2503.05613>.
- Nisan Stiennon, Long Ouyang, Jeffrey Wu, Daniel Ziegler, Ryan Lowe, Chelsea Voss, Alec Radford, Dario Amodei, and Paul F Christiano. Learning to summarize with human feedback. *Advances in neural information processing systems*, 33:3008–3021, 2020.
- Curt Tigges, Oskar J. Hollinsworth, Atticus Geiger, and Neel Nanda. Language models linearly represent sentiment. In Yonatan Belinkov, Najoung Kim, Jaap Jumelet, Hosein Mohebbi, Aaron Mueller, and Hanjie Chen (eds.), *Proceedings of the 7th BlackboxNLP Workshop: Analyzing and Interpreting Neural Networks for NLP*, pp. 58–87, Miami, Florida, US, November 2024. Association for Computational Linguistics. doi: 10.18653/v1/2024.blackboxnlp-1.5. URL <https://aclanthology.org/2024.blackboxnlp-1.5/>.

Alexander Matt Turner, Lisa Thiergart, Gavin Leech, David Udell, Juan J Vazquez, Ulisse Mini, and Monte MacDiarmid. Steering language models with activation engineering. *arXiv preprint arXiv:2308.10248*, 2023.

Xinpeng Wang, Chengzhi Hu, Paul Röttger, and Barbara Plank. Surgical, cheap, and flexible: Mitigating false refusal in language models via single vector ablation. In *The Thirteenth International Conference on Learning Representations, ICLR 2025, Singapore, April 24-28, 2025*. OpenReview.net, 2025a. URL <https://openreview.net/forum?id=SCBn8MCLwc>.

Xinyi Wang, Antonis Antoniades, Yanai Elazar, Alfonso Amayuelas, Alon Albalak, Kexun Zhang, and William Yang Wang. Generalization v.s. memorization: Tracing language models’ capabilities back to pretraining data. In *The Thirteenth International Conference on Learning Representations, ICLR 2025, Singapore, April 24-28, 2025*. OpenReview.net, 2025b. URL <https://openreview.net/forum?id=IQxBDLmVpT>.

Yufei Wang, Wanjun Zhong, Liangyou Li, Fei Mi, Xingshan Zeng, Wenyong Huang, Lifeng Shang, Xin Jiang, and Qun Liu. Aligning large language models with human: A survey. *CoRR*, abs/2307.12966, 2023. doi: 10.48550/ARXIV.2307.12966. URL <https://doi.org/10.48550/arXiv.2307.12966>.

Rowan Zellers, Ari Holtzman, Yonatan Bisk, Ali Farhadi, and Yejin Choi. HellaSwag: Can a machine really finish your sentence? In Anna Korhonen, David Traum, and Lluís Màrquez (eds.), *Proceedings of the 57th Annual Meeting of the Association for Computational Linguistics*, pp. 4791–4800, Florence, Italy, July 2019. Association for Computational Linguistics. doi: 10.18653/v1/P19-1472. URL <https://aclanthology.org/P19-1472/>.

Fred Zhang and Neel Nanda. Towards best practices of activation patching in language models: Metrics and methods. In *The Twelfth International Conference on Learning Representations, ICLR 2024, Vienna, Austria, May 7-11, 2024*. OpenReview.net, 2024. URL <https://openreview.net/forum?id=Hf17y6u9BC>.

Andy Zou, Long Phan, Sarah Li Chen, James Campbell, Phillip Guo, Richard Ren, Alexander Pan, Xuwang Yin, Mantas Mazeika, Ann-Kathrin Dombrowski, Shashwat Goel, Nathaniel Li, Michael J. Byun, Zifan Wang, Alex Mallen, Steven Basart, Sanmi Koyejo, Dawn Song, Matt Fredrikson, J. Zico Kolter, and Dan Hendrycks. Representation engineering: A top-down approach to AI transparency. *CoRR*, abs/2310.01405, 2023. doi: 10.48550/ARXIV.2310.01405. URL <https://doi.org/10.48550/arXiv.2310.01405>.

A CHAT TEMPLATES

For each considered model in our study, we resorted to the original chat template as reported either in the corresponding paper or in the HuggingFace model’s page, as shown in Table 3.

Model Family	Template
LLama3	< begin_of_text >< start_header_id >user < end_header_id >instruction< eot_id > < start_header_id >assistant< end_header_id >
Mistral	<s>[INST] instruction [/INST]
OLMo	< endoftext >< user >instruction< assistant >

Table 3: Chat templates for the model families considered in this study. Blue tokens indicate *post-instruction tokens*, as discussed in Section 2.2.

B DETAILS ON THE RUNNING ENVIRONMENT

We performed our experiments using an 8x NVIDIA A30 GPU server with 24 GB of RAM each, 764 GB of system RAM, a Double Intel Xeon Gold 6248R with a total of 96 cores, and Ubuntu Linux 20.04.6 LTS as OS.

C DETAILS ON THE MODEL CONFIGURATIONS USED FOR THE MAIN RESULTS

Table 4 reports the best model configurations used to obtain $\hat{\mathbf{r}}^*$, and the corresponding steering coefficient α , used for the results shown throughout the main paper.

Model	Math				Code			
	seed	i	ℓ^*/L	α	seed	i	ℓ^*/L	α
Llama 1B	870	-2	14/16	0.2	343	-5	14/16	0.2
Llama 3B	921	-5	23/28	0.8	689	-1	24/28	0.8
Llama 8B	245	-4	28/32	0.6	94	-4	26/32	0.2
Mistral	790	-2	24/32	0.2	237	-1	28/32	0.4
OLMo	311	-3	23/32	0.4	447	-3	26/32	0.6

Table 4: (Grid-search based) Best seed, token position (i), layer (ℓ^*/L) and steering coefficient (α) used throughout our experimental evaluation of PALRS-aligned models.

D CONFIGURATION FOR DPO ALIGNMENT

Table 5 reports the settings we used to align our used models with DPO for a comparison with PALRS.

Hyperparameter	Value
Batch size (per device)	1
Gradient accumulation steps	8
Gradient checkpointing	Enabled
Learning rate	$1e-6$
Scheduler	Linear
Optimizer	Paged AdamW (32-bit)
Training epochs	3
β coefficient	0.1 (default)

Table 5: Training hyperparameters used for DPO.

E QUALITATIVE EXAMPLES OF PALRS’S STEERING EFFECT

Figures 4-7 provide qualitative insights into the effect of model steering toward preferred behaviors obtained via PALRS.

Question: James has 30 teeth. His dentist drills 4 of them and caps 7 more teeth than he drills. What percentage of James' teeth does the dentist fix?

Expected Answer:

First find the total number of teeth the dentist caps: 4 teeth + 7 teeth = **11 teeth**

Then find the total number of teeth the dentist fixes: 11 teeth + 4 teeth = **15 teeth**

Then divide that number by the total number of teeth and multiply by 100% to find the percentage of teeth he fixes: $15 \text{ teeth} / 30 \text{ teeth} * 100\% = \mathbf{50\%}$

Baseline: James has 30 teeth. The dentist drills 4 teeth. **So, the number of teeth that the dentist fixes is $30 - 4 = 26$.**

The dentist caps 7 more teeth than he drills. So, the number of teeth that the dentist caps is $4 + 7 = 11$.

The number of teeth that the dentist fixes is **26**. The number of teeth that the dentist caps is 11. So, the percentage of teeth that the dentist fixes is **$26 / 30 * 100 = 86.67\%$**

PALRS Math: James has 30 teeth. His dentist drills 4 teeth, so he has $30 - 4 = 26$ teeth left.

The dentist caps 7 more teeth than he drills, so he caps $4 + 7 = \mathbf{11 \text{ teeth}}$.

So James has $26 - 11 = \mathbf{15 \text{ teeth}}$ that the dentist fixes.

The percentage of teeth that the dentist fixes is **$15/30 * 100\% = 50\%$**

Figure 4: Example of mathematical improvement via PALRS for Llama 3.2 1B.

Question: Mia and Emma are currently 16 years apart in age. If Mia, who is younger than Emma, is 40 years old, what's the average of their ages?

Expected Answer:

If Mia is 40 years old, Emma is $40 + 16 = \mathbf{56}$ years old.

The sum of their ages is $56 + 40 = \mathbf{96}$ years.

The average age of the two is $96/2 = \mathbf{48}$ years.

Baseline: Mia is 40 years old and Emma is **16 years old**, so the average age is $(40 + \mathbf{16})/2 = \mathbf{56 / 2 = 28}$ years.

PALRS Math: Mia is 40 years old and Emma is $40 + 16 = \mathbf{56}$ years old.

The average age of the two of them is $(40 + \mathbf{56})/2 = \mathbf{96 / 2 = 48}$ years.

Figure 5: Example of mathematical improvement via PALRS for Llama 3.2 1B.

Question:

```
def count_distinct_characters(string: str) -> int:  
    """ Given a string , find out how many distinct  
    characters (regardless of case) does it consist of  
    >>> count_distinct_characters('xyzXYZ')  
    3  
    >>> count_distinct_characters('Jerry')  
    4  
    """"
```

Baseline:

```
def count_distinct_characters(string: str) -> int:  
    # Convert the string to lowercase and remove any whitespace  
    string = string.lower().replace(" ", "")  
  
    # Create a set from the string and return the length  
    # of the set  
    return len(set(string))
```

PALRS *Code*:

```
def count_distinct_characters(string: str) -> int:  
    # Create a set to store the characters  
    char_set = set()  
  
    # Iterate through the string and add each character  
    # to the set  
    for char in string:  
        char_set.add(char.lower())  
  
    # Return the size of the set  
    return len(char_set)
```

Figure 6: Example of mathematical improvement via PALRS for Mistral 7B.

Question:

```
def string_xor(a: str, b: str) -> str:  
    """ Input are two strings a and b consisting  
    only of 1s and 0s.  
    Perform binary XOR on these inputs and return  
    result also as a string.  
    >>> string_xor('010', '110')  
    '100'  
    """
```

Baseline:

```
def string_xor(a: str, b: str) -> str:  
    result = ""  
    for i in range(len(a)):  
        if a[i] == b[i]:  
            result += "0"  
        else:  
            result += "1"  
    return result
```

PALRS *Code*:

```
def string_xor(a: str, b: str) -> str:  
    # Initialize result string  
    result = ""  
  
    # Iterate through both strings  
    for i in range(len(a)):  
        # Perform XOR operation  
        result += str(int(a[i]) ^ int(b[i]))  
  
    return result
```

Figure 7: Example of mathematical improvement via PALRS for Mistral 7B.